JOURNAL OF MATERIALS SCIENCE 32 (1997) 415–419

Varistor properties and microstructure of ZnO–BaO ceramics

J. FAN, R. FREER
Manchester Materials Science Centre, University of Manchester & UMIST, Grosvenor Street, Manchester, M1 7HS, UK

Ceramics in the system ZnO–BaO have been investigated for possible use as varistors. Specimens were prepared by the mixed oxide route, and were sintered at temperatures in the range 1000–1400 °C. The electrical properties were determined using d.c. A and impulse techniques. The ZnO–BaO ceramics have a two-phase microstructure comprising a ZnO phase and a Ba-rich grain boundary phase. Due to liquid phase sintering, the average grain sizes for the ZnO–BaO ceramics are large (typically 35–55 μm for samples sintered at 1300 °C). This results in low breakdown fields, ($\leq 1000\ V\,cm^{-1}$). The maximum non-linearity exponent obtained for ZnO–BaO ceramics (~ 14) is higher than that for binary ZnO–Bi_2O_3 ceramics. However, the high water solubility of the Ba-rich phase may restrict the use of ZnO–BaO ceramics.

1. Introduction

During the last two decades, there has been considerable progress in the development of the non-linear zinc oxide ceramics based on ZnO and small amounts of other oxide additives [1–4]. The commercial compositions for non-linear ZnO ceramics are mainly based on ZnO–Bi_2O_3 and ZnO–Pr_6O_{11} systems. Their excellent non-linear current–voltage (I–V) characteristics and the large surge-withstand capabilities have enabled them to be widely used as varistors for transient surge suppression in both electric power systems and electronic circuits.

Since the non-linearity is attributed to the grain boundary barriers [1–4], a two phase microstructure (with the ZnO-rich grains forming the primary phase and the grain boundaries the second phase) is essential for non-linear ZnO ceramics. Matsuoka *et al.* [5] reported that sintered bodies of ZnO doped with selected alkali earth metal oxides, such as BaO, also exhibit non-linear current–voltage behaviour. These additives segregate to the grain boundary to form a second phase due to their larger cation radius. Bhushan *et al.* [6] also reported that ZnO–BaO ceramics exhibit good non-linearity. Therefore, ceramics in the ZnO–BaO system appear to have potential for varistor applications. Eda *et al.* [7] noted that large ZnO grains separated from ZnO–BaO ceramics can be used as seed grains for the production of low voltage varistors. However, with the exception of these studies, very little is known about the ceramics in this system. Hence, additional investigations of the ZnO–BaO system are desirable. In this paper, we report the results of a systematic study of the non-linear current–voltage properties and microstructures of binary ZnO–BaO ceramics.

2. Experimental procedures

Samples were prepared by conventional ceramic techniques. The starting materials were analytical grade ZnO and $BaCO_3$ powders. Batches were prepared containing the following amounts of $BaCO_3$: 0.5, 1.0, 2.0 and 3.0 mol %; these yielded effective doping levels of 0.39, 0.78, 1.55 and 2.33 mol % BaO, (since the $BaCO_3$ decomposed into BaO during sintering [8]). The powders were mixed, ball milled for 6 h and dried. Granules were obtained by passing the dried powders through a screen having an aperture mesh of nominally 0.3 mm. Samples in the form of discs (16 mm in diameter and 3 mm in thickness) were then pressed by a single action, uniaxial press at 80 MPa. The green compacts were sintered in air for 1 h at different temperatures in the range of 1000–1400 °C. The heating rate and cooling rate were 120 °C per h and 150 °C per h, respectively.

The sintered densities of the samples were determined using the Archimedes method. The reference theoretical density was taken to be $5.61\ g\,cm^{-3}$, that of pure ZnO. A Philips PW1710 diffractometer in conjunction with a horizontal goniometer was used for X-ray analysis to identify the phases present. The microstructures of the sintered samples were examined using optical and scanning electron microscopy (SEM) (Philips 505 with an energy dispersive X-ray analytical facility, EDX). For SEM examinations the specimens were polished, and slightly etched with 5% dilute hydrochloric acid. The average grain size was determined from photomicrographs, using Mendelson's intercept method [9].

Before electrical measurements, both surfaces of the pellets were lapped to give a final thickness of 2.50 mm. Electrical contacts were applied to both surfaces using conducting silver paint. The

0022–2461

current–voltage (I–V) characteristics of the samples were measured at room temperature using a variable d.c. power supply (Bradenburg 475R) up to 5 mA. To prevent overheating, measurements at higher current levels (> 5 mA) were made using a laboratory-built, impulse I–V measuring instrument; the typical current wave shape was 8×20 μs. The non-linearity exponents (α) were determined from I–V data, between current densities of 0.1–1 mA cm^{-2}. Further details about the methods used to determine the electrical properties are presented elsewhere [10, 11].

3. Results and discussion

3.1. Densification

Fig. 1 shows the sintered densities of samples in the ZnO–BaO system as a function of the sintering temperature. It can be seen that at a constant sintering temperature, the sintered density of the doped samples decreased with an increase in the BaO content. At a constant doping level, the density increased as the sintering temperature increased from 1000–1100 °C (achieving the maximum value at 1100 °C); as the sintering temperature was increased further the density decreased, almost linearly. This trend is different from that of the nominally "pure" (i.e., undoped) ZnO ceramics, whose density increased with increasing sintering temperature up to 1300 °C, achieving the maximum value at 1300 °C (Fig. 1). Therefore, for the range of doping levels investigated, 1100 °C appears to be the optimum sintering temperature for the densification of ZnO–BaO ceramics. The highest density of 5.45 g cm^{-3} (equivalent to 97.1% of the theoretical density of ZnO) was obtained for samples containing 0.39 mol % BaO, sintered at 1100 °C.

3.2. Microstructures

Fig. 2(a and b) shows typical micrographs of the sintered surface for the samples doped with 0.39 mol % and 2.33 mol % BaO sintered at 1300 °C. The primary grains were variable in shape, but generally they became more rounded in specimens with higher BaO contents. The relationship between the average grain size and the level of BaO doping, for the samples sintered at 1300 °C, is shown in Fig. 3. It can be seen that the average grain sizes for doped samples are larger than that of the undoped ZnO ceramics, and that the average grain sizes increased with BaO

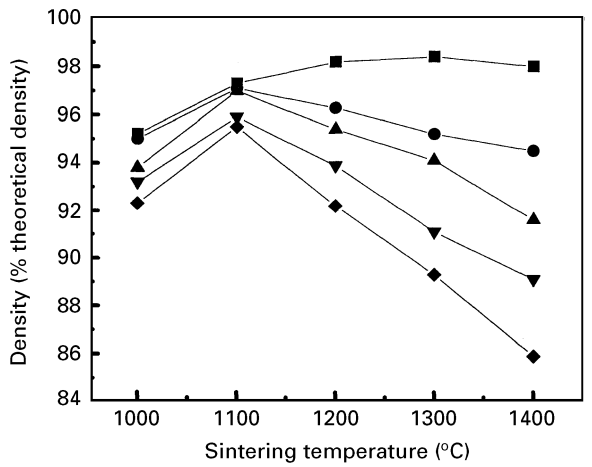

Figure 1 Density of ZnO–BaO ceramics as a function of sintering temperature, (typical standard deviation: ± 0.2%). The samples invesitgated were; (■) Undoped ZnO (0% BaO), (●) 0.39 mol % BaO, (▲) 0.78 mol % BaO, (▼) 1.55 mol % BaO and (◆) 2.33 mol % BaO.

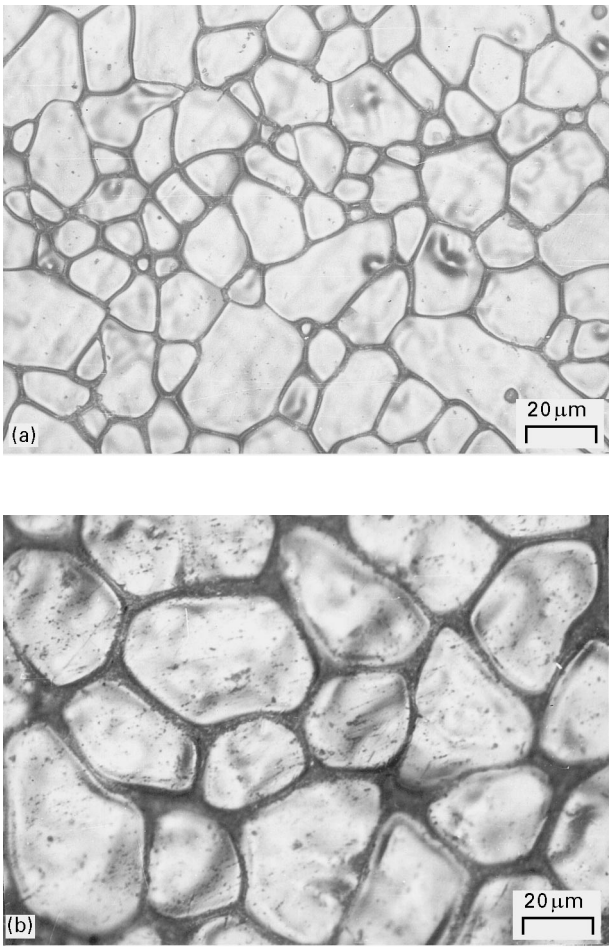

Figure 2 Typical micrographs of ZnO–BaO samples sintered at 1300 °C. (a) containing 0.39 mol % BaO; (b) containing 2.33 mol % BaO.

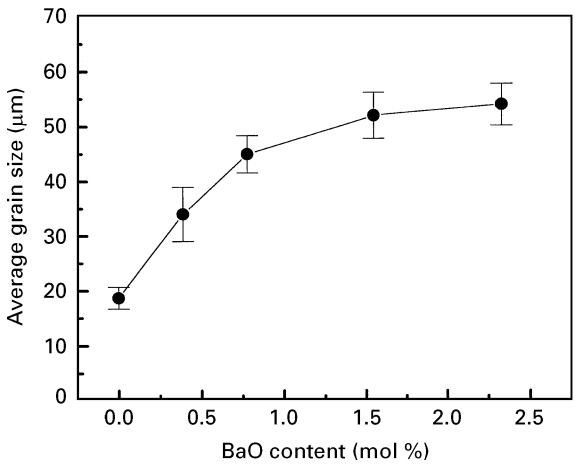

Figure 3 The relationship between the average grain size and BaO content for the samples sintered at 1300 °C (typical standard deviation: ± 10%).

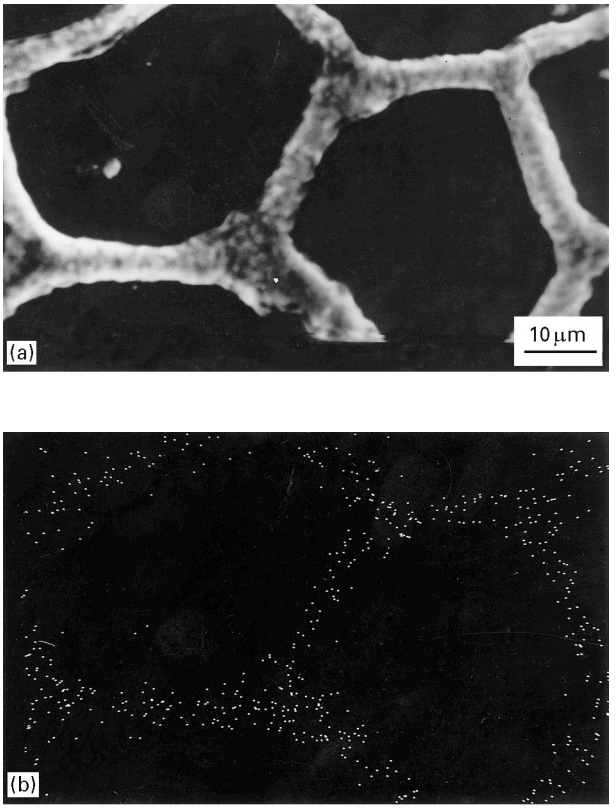

Figure 4 Typical SEM micrographs of a sample doped with 0.78 mol % BaO, sintered at 1300 °C. (a) SEM micrograph; (b) EDS elemental scan for Ba.

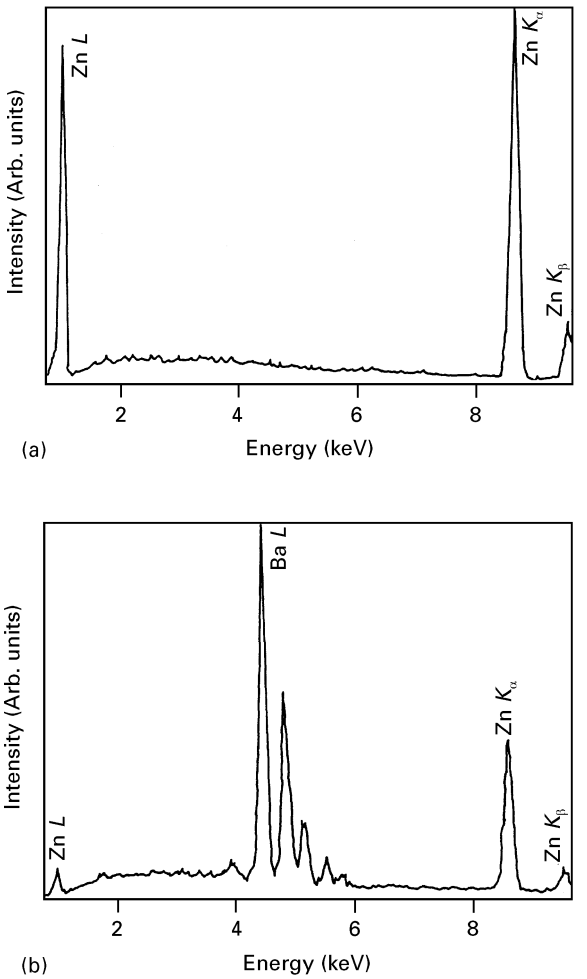

Figure 5 EDS spectra for ZnO–BaO ceramics: (a) Grain; (b) Grain boundary.

content. For the addition of 0–0.78 mol % BaO, the increase of grain size was rapid, changing by approximately a factor of 2. Beyond 0.78 mol % BaO, the grain size increased at a slower rate. For samples prepared with 2.33 mol % BaO, the average grain size was 55 ± 6 μm, which is approximately three times larger than that of the undoped ZnO samples. This extensive grain growth may be due to the presence of a liquid phase in the doped samples during sintering [8]. From Fig. 2(a and b) it can also be seen that the individual grains are surrounded by a grain boundary phase. This intergranular phase could be formed from a liquid phase during cooling. Furthermore, it is apparent from Fig. 2(a and b) that in the samples with a higher BaO content, the boundary phase is wider and the grains are more rounded, which suggests complete wetting of grain boundaries by a liquid phase and that direct grain growth via a solid–solid contact mechanism is unlikely [8].

Further details of the microstructure are revealed in Fig. 4a, which is a typical SEM micrograph of a sample doped with 0.78 mol % BaO and sintered at 1300 °C. It can be seen that there are two phases within the binary ZnO–BaO ceramics, i.e., the primary grains and an intergranular phase. From an EDX elemental scan for Ba in the same region (Fig. 4b), it is clear that Ba is concentrated in the grain boundary regions. EDX spectra shown in Fig. 5(a and b) confirm that the grains are almost exclusively ZnO with no more than a trace of Ba (Fig. 5a), and that the grain boundary phase is Ba-rich, containing an appreciable amount of Zn (Fig. 5b). X-ray diffraction analysis of these samples further confirmed that the two crystalline phases are ZnO and BaO. Hence, the grain boundaries have the structure of BaO and chemically are predominantly BaO containing Zn.

Considering the large size of Ba ions, the above results are consistent with the very low solubility of BaO in ZnO [13]. During sintering the Ba^{2+}, which has a much larger cation radius (0.134 nm) than Zn^{2+} (0.074 nm), could only have a very limited solubility in the ZnO lattice, so it mainly segregates to the grain boundary. Thus the presence of the Ba-rich phase enhances grain growth of ZnO during sintering, and leads to a two phase microstructure in the ZnO–BaO ceramics.

3.3. Non-linear current–voltage (*I–V*) characteristics

Non-linear current–voltage (*I–V*) characteristics were obtained for the ZnO samples prepared with BaO additions sintered at temperatures in the range of 1000–1400 °C. The non-linearity exponents (α) for these samples are shown in Fig. 6. It is clear that the non-linearity exponent (α) was strongly influenced by the Ba content and the sintering temperature. For all doping levels, samples sintered at low temperatures (≤ 1100 °C), have low α values (< 5). As the sintering temperature was increased, the α value increased,

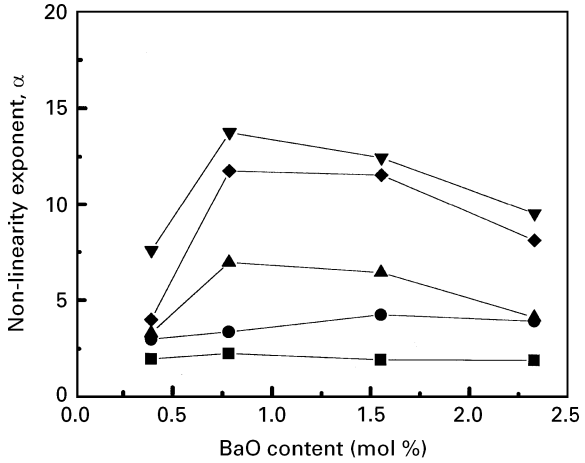

Figure 6 Non-linearity exponent (α) for ZnO–BaO ceramics as a function of BaO contents for samples sintered at temperature of (■) 1000 °C, (●) 1100 °C, (▲) 1200 °C, (▼) 1300 °C and (◆) 1400 °C.

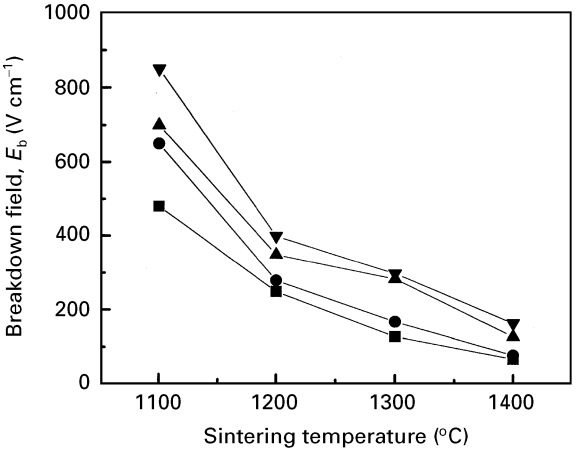

Figure 8 Breakdown field (E_b) for the ZnO–BaO ceramics as a function of sintering temperature. The compositions investigated were; (■) 0.39 mol % BaO, (●) 0.78 mol % BaO, (▲) 1.55 mol % BaO and (▼) 2.33 mol % BaO.

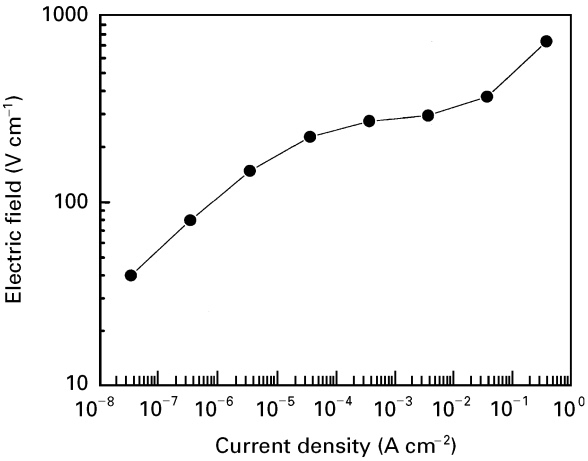

Figure 7 Electric field (E)-current density (J) characteristics for a sample doped with 0.78 mol % BaO, sintered at 1300 °C.

achieving a maximum for samples sintered at 1300 °C. Increasing the sintering temperature further to 1400 °C, caused the α values to drop slightly. Therefore, to achieve the optimum non-linearity, the sintering temperature for ZnO–BaO ceramics must be above 1200 °C. At a constant sintering temperature ($\geq$ 1200 °C), the samples doped with $\geq$ 0.78 mol % BaO have higher non-linearity exponents than the samples doped with 0.39 mol % BaO. This may be because the low doping level (0.39 mol % BaO) is not sufficient to form adequate Schottky barriers at the grain boundaries, which are responsible for the non-ohmic behaviour of ZnO varistors [1–4].

Within this study, the highest α value of 13.8 was obtained for the samples doped with 0.78 mol % BaO and sintered at 1300 °C. This value is higher than that reported for the binary ZnO–Bi_2O_3 ceramics, which never exceed 10 [3]. Fig. 7 shows the typical electric field-current density (E–J) characteristics at room temperature for a sample doped with 0.78 mol % BaO and sintered at 1300 °C. It may be seen that although it has the highest α value, the non-linear region (the central flat region of the curve in Fig. 7) is rather narrow, extending over only 2 to 3 orders of magnitude of current density. This suggests that in general, binary ZnO–BaO ceramics have restricted non-linear current–voltage characteristics, possibly because the Schottky barriers formed in this binary system are inferior to these in ZnO–Bi_2O_3 based ceramics.

Fig. 8 shows the breakdown field (E_b) of ZnO–BaO ceramics as a function of sintering temperature (between 1100–1400 °C). At a constant BaO content, the breakdown field of the samples decreased rapidly as the sintering temperature increased from 1100–1200 °C. With further increase in sintering temperature the rate of fall of E_b reduced. At a constant sintering temperature the E_b value increased with increasing BaO content; this could be due to the thicker grain boundary phase formed in samples prepared with higher BaO doping levels. Overall, the breakdown field for the binary ZnO–BaO ceramics is low (< 1000 V cm^{-1}). This must be due to their large grain size (typically 35–55 μm), so that there are less barriers in series connection within a unit thickness.

From the above results, it is obvious that the behaviour of binary ZnO–BaO ceramics is similar to that of the binary ZnO–Bi_2O_3 ceramics. The non-linearity developed in these two systems can be attributed to the unique two phase microstructure. Therefore, the ZnO–BaO ceramics are potential varistor materials. However, a factor which merits attention is that the Ba-rich phase in the binary ZnO–BaO ceramics is susceptible to attack by moisture and indeed easily dissolves in water. When the ceramics are stored in air, moisture readily enters the sintered bodies and damages the grain boundary. Evidence of this problem was observed during the present investigation. This behaviour may be interpreted in terms of the high water solubility of BaO [12]. Hence, the binary ZnO–BaO ceramics may have a limited commercial value. However, this high water solubility can be an advantage since it enables the easy separation of the large ZnO grains from ZnO–BaO ceramics to provide ZnO seed grains for the production of low-voltage ZnO varistors [7]. Such components specifically need the larger grain sizes.

4. Conclusions

(1) ZnO–BaO ceramics are two phase polycrystalline ceramics. The microstructure of ZnO–BaO ceramics consists of ZnO grains and a Ba-rich intergranular phase.

(2) At a constant sintering temperature, the density of ZnO–BaO ceramics decreases as the Ba-doping level increases. The optimum sintering temperature for ZnO–BaO ceramics was found to be 1100 °C. At this sintering temperature the density of ZnO–BaO ceramics achieved maximum values ($\geq 95\%$ dense).

(3) The ZnO–BaO ceramics exhibited non-linear current–voltage (I–V) characteristics. The highest α value of 13.8 was obtained with samples prepared with 0.78 mol % BaO, sintered at 1300 °C.

(4) The breakdown field (E_b) for the ZnO–BaO ceramics was low ($\leq 1000\ V\ cm^{-1}$). This is probably due to the large grain size of the ZnO–BaO ceramics.

(5) The high water solubility of the Ba-rich phase restricts the use of ZnO–BaO ceramics. However, it may provide a means of extracting large ZnO grains from the ZnO–BaO ceramics, which can then be used as seed grains for the preparation of low-voltage ZnO varistors.

References

1. M. MATSUOKA, in "Advances in Ceramics", Vol. 1, edited by L. M. Levinson and D. Hill (The American Ceramic Society, Columbus, OH, 1981) 290.
2. L. M. LEVINSON and H. R. PHILIPP, *Amer. Ceram. Soc. Bull.* **65** (1986) 639.
3. K. EDA, *IEEE Electric Insul. Mag.* **5** (1989) 28.
4. K. MUKAE, K. TSUDA and I. NAGASAWA, *Jpn. J. Appl. Phys.* **16** (1977) 1361.
5. M. MATSUOKA, T. MAUYAMA and Y. IIDA, *ibid* **8** (1969) 1275.
6. B. BHUSHAN, S. C. KASHYAP and K. L. CHOPRA, *Appl. Phys. Lett.* **38** (1981) 160.
7. K. EDA, M. INADA and M. MATSUOKA, *J. Appl. Phys.* **54** (1983) 1095.
8. K. UEMATSU, T. MORIMOTO, Z. KATO, N. UCHIDA and K. SAITO, *J. Amer. Ceram. Soc.* **72** (1989) 1070.
9. M. I. MENDELSON, *ibid* **52** (1969) 443.
10. J. FAN and R. FREER, *J. Mater. Sci.* **28** (1993) 1391.
11. *Idem.*, *J. Appl. Phys.* **77** (1995) 4795.
12. "Handbook of Chemistry and Physics", 70th Edn (CRC Press Inc., Boca Raton, FL, 1989) B-68.
13. K. UEMATSU, T. MORIMOTO, Z. KATO, N. UCHIDA and K. SAITO, *J. Mater. Sci. Lett.* **6** (1987) 1285.

Received 23 February
and accepted 5 July 1996